Ultrasound in Med. & Biol., Vol. 42, No. 1, pp. 299–307, 2016

0301-5629/$ - see front matter

http://dx.doi.org/10.1016/j.ultrasmedbio.2015.08.017

● *Original Contribution*

THERMOCHROMIC PHANTOM AND MEASUREMENT PROTOCOL FOR QUALITATIVE ANALYSIS OF ULTRASOUND PHYSIOTHERAPY SYSTEMS

Rejane M. Costa,* André V. Alvarenga,† Rodrigo P. B. Costa-Felix,† Thaís P. Omena,* Marco A. von Krüger,* and Wagner C. A. Pereira*

*Biomedical Engineering Program, COPPE, Federal University of Rio de Janeiro, Rio de Janeiro, Brazil; and †Laboratory of Ultrasound/National Institute of Metrology, Quality, and Technology (Inmetro), Duque de Caxias, Rio de Janeiro, Brazil

(*Received* 6 *April* 2015; *revised* 18 *August* 2015; *in final form* 26 *August* 2015)

Abstract—Thermochromic test bodies are promising tools for qualitatively evaluating the acoustic output of ultrasound physiotherapy systems. Here, a novel phantom, made of silicone mixed with thermochromic powder material, was developed. Additionally, a procedure was developed to evaluate the stability and homogeneity of the phantom in a metrologic and statistical base. Twelve phantoms were divided into three groups. Each group was insonated by a different transducer. An effective intensity of 1.0 W/cm^2 was applied to each phantom; two operators performed the procedure three times in all phantoms. The heated area was measured after image processing. No statistical difference was observed in the heated areas for different samples or in the results for different operators. The heated areas obtained using each transducer were statistically different, indicating that the thermochromic phantom samples had sufficient sensitivity to represent the heated areas of different ultrasonic transducers. Combined with the evaluation procedure, the phantom provides an approach not previously described in the literature. The proposed approach can be used to quickly assess changes in ultrasonic beam cross-sectional shape during the lifetime of ultrasound physiotherapy systems. (E-mail: avalvarenga@inmetro.gov.br or http://www.inmetro.gov.br) © **2016 World Federation for Ultrasound in Medicine & Biology.**

Key Words: **Ultrasound, Physiotherapy, Thermochromic phantom, Metrology.**

INTRODUCTION

Therapeutic ultrasound is widely used in physiotherapy treatment protocols because of its thermal and mechanical effects on biological tissues (Merrick et al. 2003; Speed 2001). The technical standard IEC 61689 (International Electrotechnical Commission [IEC] 2013a) describes, in a wide sense, the criteria to be considered while evaluating the performance and tolerability of physiotherapy equipment. The main quantities whose measurement methods and performance requirements are governed by this standard are effective radiating area, acoustic power and acoustic intensity. The standard technique for measuring these quantities is expensive and complex because it requires an acoustic tank equipped with a positioning system for scanning the acoustic field and a radiation force balance to perform power measurement. All existing measurement methods are intended to be used by metrology laboratories (IEC 2013a).

A different approach is proposed in the technical specification IEC TS 62462 (IEC 2007), which establishes alternative methods for checking the performance of ultrasound physiotherapy devices during their lifetime. This specification describes qualitative methods that final users (*e.g.,* physical therapist) should perform periodically to ensure, with a considerable margin of safety, that the equipment remains reliable after commissioning. According to IEC TS 62462, previous quantitative assessment is necessary to establish a baseline for future qualitative analyses (IEC 2007).

The previous evaluation of ultrasonic equipment used in physical therapy in terms of the values of its output quantities according to, for instance, IEC 61689 (IEC 2013a), does not necessarily guarantee its consistent behavior throughout its lifetime. This fact has been validated by many studies conducted in several countries (Artho et al. 2002; Ferrari et al. 2010; Guirro and Santos

Address correspondence to: André V. Alvarenga, Laboratory of Ultrasound, Division of Acoustic and Vibration Metrology, Directory of Scientific and Industrial Metrology, INMETRO, Av. N. Sra. das Gracas, 50-Xerem, 25250-020 Duque de Caxias, Rio de Janeiro, Brazil. E-mail: avalvarenga@inmetro.gov.br or http://www.inmetro.gov.br

2002; Hekkenberg et al. 1986; Ishikawa et al. 2002; Pye and Milford 1994; Schabrun et al. 2008), highlighting the importance of the periodic verification of therapeutic ultrasound devices. From a clinical point of view, the use of devices that conform to technical standards and are in reliable operating condition is ultimately the basis for reliable treatment.

Measurement methods described in IEC TS 62462 cover the necessity of performing periodic tests on ultrasonic devices. However, new, fast and reliable qualitative methods are under study. A promising research field is the study of thermochromic materials, typically used in the construction of test bodies (*e.g.*, phantoms, sheets or tiles). This type of material is susceptible to heating, resulting in color changes that create tiny spots. Depending on the construction of a test body and the temperature gradient within it, it is possible to observe a color change on its surface. When an ultrasonic field irradiates a material, the temperature rises because of absorption. Therefore, considering the absorption properties of the test body constructed using a thermochromic material, one could expect to visualize a color change related to the temporal-average intensity derived from the ultrasonic pressure field. Cook and Werchan (1971) presented the first work on ultrasound field mapping by direct radiation on a thermochromic sheet. Other studies have reported the use of these materials, wherein the heating pattern of the acoustic field is visualized in a plane parallel to the transducer face (and, therefore, perpendicular to the propagation beam direction) (Gómez et al. 2006; Macedo et al. 2003; Martin and Fernandez 1997). Butterworth et al. (2012) developed a reusable absorber composed of polyurethane layers and thermochromic material that changes its color starting from 30°C to evaluate therapeutic ultrasound equipment. They produced two types of the reusable absorber: a double-layer type, in which the thermochromic material was added to the layer with the highest acoustic absorption, and a triple-layer type, in which the pigment was added to the intermediate layer. The results obtained with the latter were a good qualitative match to measurements made by hydrophone scanning over the same transducers.

In this article, we propose a new test body (phantom) to be used in the biologically relevant hyperthermia temperature range, that is, above 45°C. The phantom is made of a simpler matrix (compared with those described in the literature) that combines silicone with thermochromic powder material; the phantom can be easily prepared and is reusable. Additionally, a procedure is developed to evaluate the short-term stability and homogeneity of the phantom in a metrologic and statistical base. Combined with the evaluation procedure, the phantom provides a new approach that has not been reported in the literature so far. The applicability of the proposed approach can be extended to clinical practice, for instance, as an alternative or addition to those described in IEC TS 62462 (IEC 2007).

METHODS

Thermochromic material

The phantoms were prepared using silicone RTV 615 (General Electric), which contains a solution of two products, RTV 615A and RTV 615B. A small amount of thermochromic material with a color-variation temperature of 45°C (ChromaZone, Thermographic Measurements, Honiton, UK) was mixed with the silicone. RTV 615 B was mixed with the thermochromic material powder, and then, the mixture was sieved to avoid formation of an agglomerate of the thermochromic powder. The sieved material was further mixed with RTV 615A, and the mixture was degassed in a vacuum chamber for approximately 1 h. The degassed mixture was placed in molds over a leveled surface for drying and solidification for approximately 12 h at room temperature (25°C). Twelve samples were produced for this study, all 4.75 ± 0.05 g in weight, 3.7 ± 0.1 cm in diameter and 0.40 ± 0.05 cm in thickness. The attenuation (1.4 ± 0.1 dB/cm at 1 MHz) and speed of sound (1016 ± 6 m/s) were determined at Inmetro's Laboratory of Ultrasound.

Ultrasound system

Two 3-MHz ultrasound physiotherapy treatment heads (named transducers A and B, both with a nominal diameter of 25 mm) and a 3.5-MHz circular single-element transducer with a nominal diameter of 25.4 mm (A380 S, Panametrics-Olympus-NDT, Waltham, MA, USA; named transducer C) were used in the study. Some physical therapy systems have unstable voltage output, so all transducers were driven by a function generator (AFG 3252, Tektronix, Beaverton, OR, USA) connected to a radiofrequency (RF) amplifier (E&I 3200L, Electronics and Innovation, Rochester, NY, USA). The system was calibrated to generate an intensity of 1.0 W/cm^2 for each nominal central frequency of the transducers. The effective radiating area was determined by undertaking a raster scan of the acoustic field in a plane perpendicular to the beam alignment axis, at a distance of 3 mm from the output face of the treatment head, using a hydrophone, according to the procedure specified in IEC 61689 (IEC 2013a). The power was calibrated using a radiation force balance according to IEC 61161 (IEC 2013b). All uncertainties were determined according to JCGM 100:2008 (Bureau International des Poids et Mesures [BIPM] 2008).

According to Blackstock (1966) and Beyer (1960), the total harmonic distortion is less than –25 dB for an

effective intensity of 1.0 W/cm^2 and a propagation distance of 14 mm (between the transducer face and the phantom), indicating the absence of non-linear propagation during the heating experiments.

Thermal activation, image generation, acquisition and processing

The proposed phantom is intended to be used for visual inspection without the mandatory aid of any camera or image capture device. However, to accurately quantify the thermal effect, that is, the color change over the phantom surface, a protocol for thermal activation and image evaluation was developed. Image evaluation comprised a capture procedure and subsequent image processing based on morphologic operators. Thermochromic phantom images were captured using a digital camera at the time instants 0 and 30 s. This time interval was defined empirically to produce the desired heating pattern and preserve the reversibility of the thermochromic pigment. The images were collected using the following procedure:

1. The digital camera is positioned on the tripod, ensuring that the height is fixed throughout the experiments (it is positioned 15 cm away from the phantom).
2. A plastic adapter is coupled to the transducer (Fig. 1), so that the phantom is 14 mm away from the transducer face; care is taken to orient the transducer in the same manner for every repetition.
3. The gap between the adapter and transducer is filled with distilled water at a temperature of 21°C (maximum variation of ±0.1°C). The water layer provides ultrasonic coupling between the transducer face and phantom and also insulates the phantom from the conductive (non-acoustic) heating effects.

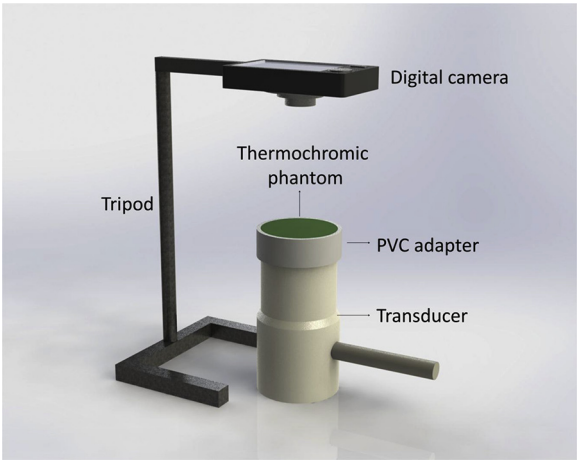

Fig. 1. Schematic of the experimental setup.

4. The thermochromic phantom is placed on the top of the adapter, making sure that there are no air bubbles under the phantom.
5. One initial picture (reference image) is taken at 0 s.
6. The generator is turned on.
7. After 30 s, the generator is turned off, and a second picture (final image) is taken.

An image processing procedure, developed in MATLAB (The Mathworks, Natick, MA, USA), was used to determine the region and respective geometric area produced by the heating. The image processing procedure, based on a morphologic filter (Soille 1999), follows these steps:

1. Images acquired at 0 s (reference) and 30 s (final) are converted to gray scale.
2. The reference image is segmented using a set of morphologic filters to detect the surface area of the thermochromic phantom (without color change).
3. The pixel size is determined based on the actual dimensions of the thermochromic phantom.
4. The heated region is segmented using an image produced by subtracting the reference image from the final image and a sequence of morphologic filters.
5. The area of the heated region is determined (in square centimeters).

Regular fluorescent light bulbs were used to illuminate the room where the experiments were performed. It is worth emphasizing that as the analysis is relative, the type of illumination is not a major issue. However, considering the quantitative analysis presented here, it is important to carry out the measurement under the same light conditions to ensure adequate comparison between images acquired at different times. If the phantom is used for visual inspection without the aid of any image capture device or image processing, variations in light conditions will not be significant.

Statistical analysis

A procedure was defined to evaluate the homogeneity among different samples of the thermochromic phantom, as well as the effect of the operator on the measurement. First, the 12 phantoms were randomly separated into three groups with four samples each. Each group was used with each one of the three transducers used in this study: transducer A (samples A1–A4), transducer B (samples B1–B4) and transducer C (samples C1–C4). Two operators repeated the image capture protocol three times (rep1, rep2 and rep3) for each group of phantoms and the respective transducer. It is worth emphasizing that the experiments were completely independent; disassembly and re-assembly

were performed between repetitions and the samples inside a group were tested alternately.

The homogeneity among samples from the same group (intragroup test) was evaluated with the χ^2 test ($\alpha = 0.05$) for each operator independently. The χ^2 test is used to assess whether different samples are sufficiently homogeneous and stable to reproduce the heated area. Thus, considering that the samples were homogeneous, the results obtained within each group were combined. The *F*-test was applied to assess whether the results for each operator had homogenous variance, and the *t*-test for the difference between two means ($\alpha = 0.05$) was used to analyze whether there was a statistical difference between the results achieved by each operator (intergroup for different operators). Finally, the results achieved by each operator were combined, yielding an average result for each transducer (overall intergroup).

Overlap area ratio

The overlap area ratio is used to assess the superposition degree among areas from the three different repetitions for the same sample, yielding an estimate of the repeatability of the obtained area shape. The overlap ratio is calculated as

$$overlap\ ratio = \frac{Area_{rep1} \cap Area_{rep2} \cap Area_{rep3}}{Area_{rep1} \cup Area_{rep2} \cup Area_{rep3}} \quad (1)$$

where $Area_{repn}$ represents the area of the heated region at repetition *n* for a specific sample, and symbols $\cap$ and $\cup$ represent the intersection and union among the areas, respectively. This quantity is assessed for each sample in each group (A–C) and for each operator.

RESULTS

Effective radiating area (A_{ER}), output power (P) and effective intensity (I_e) values for the three transducers studied are summarized in Table 1, with the respective expanded uncertainties (U). Examples of mappings performed to determine the effective radiating area are illustrated in Figure 2.

Table 1. Effective radiating area (A_{ER}), output power (P) and effective intensity (I_e) for the three transducers studied, with the respective expanded uncertainties U ($k = 2$)

Transducer	A_{ER} (cm^2)	U_A (cm^2)	P (W)	U_P (W)	I_e (W/cm^2)	U_I (W/cm^2)
A	2.71	0.26	2.700	0.090	1.00	0.10
B	3.03	0.12	3.032	0.080	1.000	0.050
C	4.60	0.18	4.57	0.11	0.993	0.050

As described under Statistical Analysis, two operators (1 and 2) repeated three times (rep1, rep2, rep3) the heating experiments with the different phantom samples (A1–A4, B1–B4, C1–C4). To illustrate qualitatively the homogeneity among different samples of the thermochromic phantom, as well as between operators on the measurement, examples of heating patterns obtained for different samples and operators are provided in Figures 3–5.

In Figure 3a, one can see the heated area produced by transducer C at the second repetition (rep2) performed by operator 1, using sample C3. For the same sample C3, the heated area obtained at the first repetition (rep1) performed by operator 2 is illustrated in Figure 3b. An example of the heated area obtained by operator 1 using a different sample (C4) is found in Figure 3c. The area contours obtained from the three repetitions performed by operators 1 (white, red, and green) and 2 (blue, yellow, and cyan) for sample C3 are illustrated in Figure 3d. In Figure 3e, the area contours achieved by operator 1 using different samples (C3: *white, red and green*; C4: *blue, yellow and cyan*) can be seen.

Considering transducer B, one can see in Figure 4a the heated area produced at the third repetition performed by operator 1, using sample B4. For the same sample B4, the heated area obtained at the first repetition performed by operator 2 is illustrated in Figure 4b. An example of the heated area produced by a different sample (B3) is provided in Figure 4c. The area contours obtained from the three repetitions performed by operators 1 (*white, red and green*) and 2 (*blue, yellow and cyan*) for sample B4 are illustrated in Figure 4d. The area contours achieved by operator 1 using different samples (B3: *white, red and green*; B4: *blue, yellow and cyan*) are presented in Figure 4e.

Figure 5a illustrates the heated area produced by transducer A at the first repetition (rep1) performed by operator 1, using sample A4. For the same sample A4, the heated area obtained at the third repetition performed by operator 2 is illustrated in Figure 5b. An example of the heated area produced by a different sample (A3) is provided in Figure 5c. The area contours obtained from the three repetitions performed by operators 1 (*white, red and green*) and 2 (*blue, yellow and cyan*) for sample A4 are in Figure 5d. Finally, the area contours achieved by operator 1 using different samples (A3: *white, red and green*; A4: *blue, yellow and cyan*) are presented in Figure 5e.

Figure 6 illustrates the relationship between the heated area values and respective effective radiating areas.

The heated area values for all samples, with the respective overlap ratios, are summarized in Table 2. χ^2 tests revealed that all samples from the same group

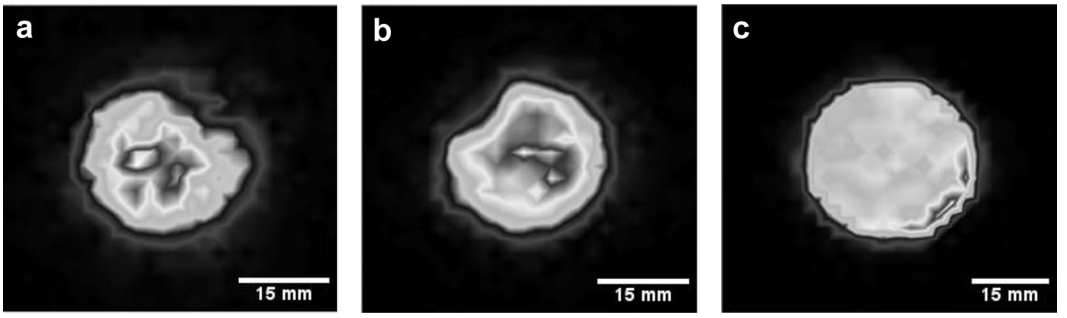

Fig. 2. Examples of the beam cross-sectional area 0.3 cm from the face of the treatment heads: (a) transducer A, (b) transducer B, (c) transducer C. Measurements were performed according to IEC 61689 (IEC 2013a).

(intragroup test) were homogeneous ($p < 0.01$) for each operator independently. Hence, it was possible to calculate the mean area and respective standard deviation among the samples from the same group for each operator. These results are summarized in Table 3; the *F*-test indicated that the variances between the two operators were homogeneous (intergroup for different operators). Consequently, the variances were combined, and the *t*-test for the difference between two means ($\alpha = 0.05$) indicated no statistical difference between the results achieved by each operator, that is, the overall intergroup (Table 3). Finally, the results achieved by each operator were combined, and the final mean area for each transducer was determined with its respective standard deviation at intermediate measurement precision (Table 4). For the definition of "intermediate measurement precision," please refer to JCGM 200:2012 (BIPM 2012).

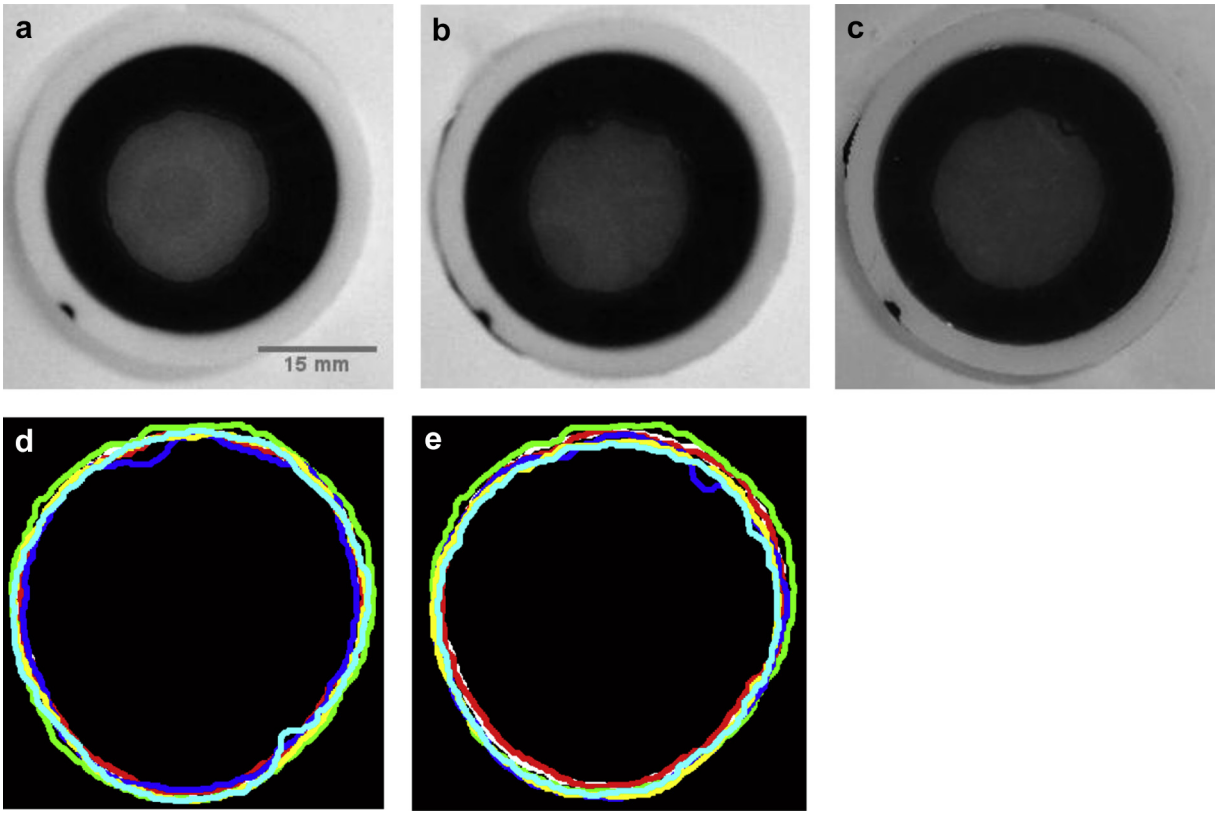

Fig. 3. (a) Example of a region heated in sample C3 achieved by operator 1, at second repetition, with transducer C. (b) Example of result obtained by operator 2, for the same sample C3. (c) Example of the heated area produced by a different sample (C4). (d) Area contours obtained from the three repetitions performed by operators 1 (*white, red and green*) and 2 (*blue, yellow and cyan*) for sample C3. (e) Area contours obtained by operator 1 using different samples (C3: *white, red and green*; C4: *blue, yellow and cyan*).

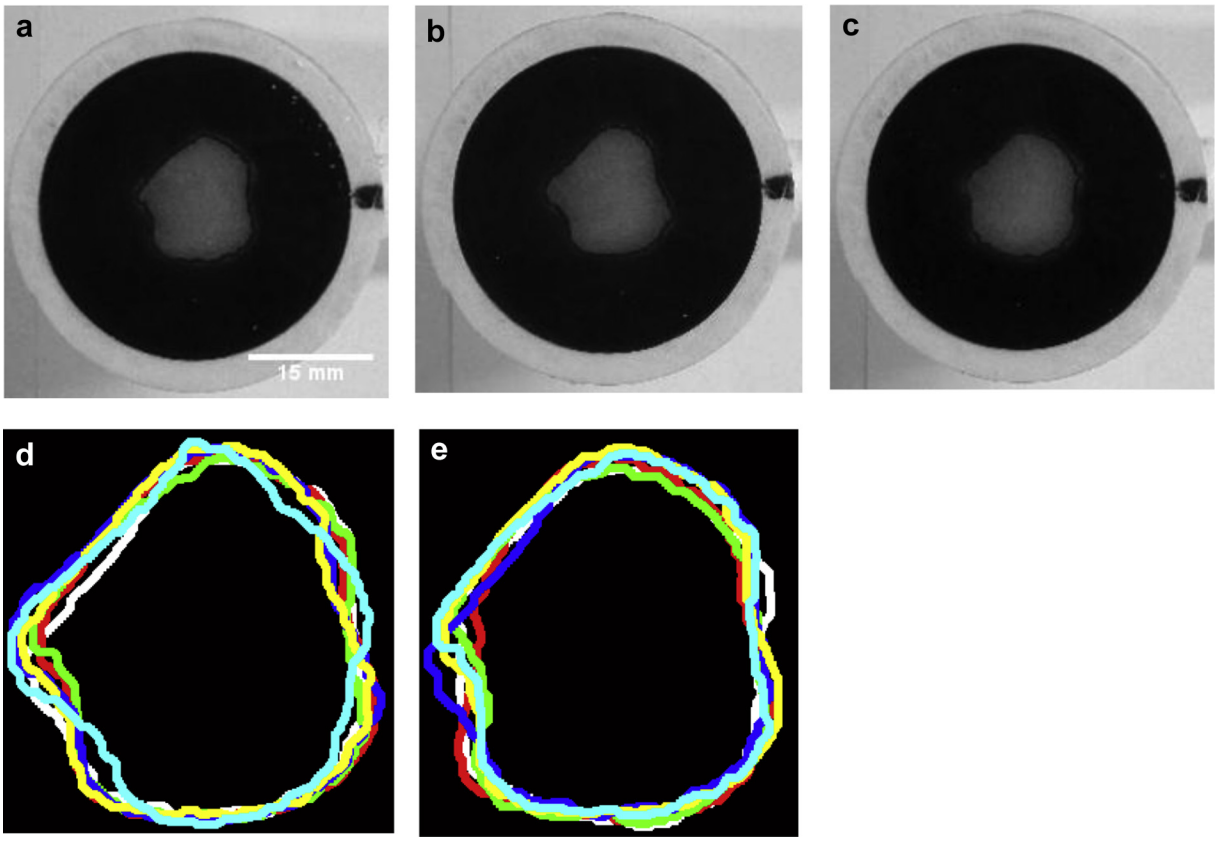

Fig. 4. (a) Example of a region heated in sample B4 achieved by operator 1, at second repetition, with transducer B. (b) Example of result obtained by operator 2 for the same sample B4. (c) Example of the heated area produced by a different sample (B3). (d) Area contours obtained from the three repetitions performed by operators 1 (white, red and green) and 2 (*blue, yellow and cyan*) for sample B4. (e) Area contours obtained by operator 1 using different samples (B3: *white, red and green*; B4: *blue, yellow and cyan*).

DISCUSSION AND CONCLUSIONS

Transducer C gives a regular circular pattern, and the results obtained using different thermochromic phantom samples are quite similar (Fig. 3e); this similarity is confirmed by the high values for overlap ratio (>0.88). Moreover, transducer C yields the largest A_{ER} value and heated area. As previously mentioned, this transducer is not a typical physiotherapy treatment head, but an NDT transducer.

Transducer B does not give a circular heating pattern, which is in agreement with its respective beam cross-sectional area ("bitten cookie" pattern in Fig. 2b). One can also observe the reproduction of this heating pattern at different repetitions for different operators (Fig. 4d) and also for different thermochromic phantom samples (Fig. 4e). Moreover, despite the non-circular heating pattern, the values of the overlap ratio are higher than 0.83. It is noteworthy that care was taken to orient the transducer in the same manner for every repetition. Transducer A gives the lowest heated area, as well as the lowest A_{ER} value.

In assessing transducer A, one can note a small intensity reduction in the top right region of the beam cross-sectional area (Fig. 2a). Despite this reduction in intensity, area reduction does not appear clearly in the heated region; the heated area seems to have a slightly oval shape (Fig. 5). By comparing this result with that obtained for transducer B, one could also expect the heated area to have a "bitten cookie" pattern (Fig. 2b). However, it is clear that the intensity reduction in the top right region of transducer A is less intense than that observed for transducer B. In addition, the beam cross-sectional area obtained by mapping the transducer using a hydrophone has higher resolution than the area obtained by using the thermochromic phantom.

It can be observed that the overlap ratio values for transducer A are smaller than those for the other two transducers; in addition, the standard deviation of the heated area for transducer A is higher. Assessment of the A_{ER} values listed in Table 1 reveals that transducer A has higher expanded uncertainty than the other transducers. This is an indication that the repeated

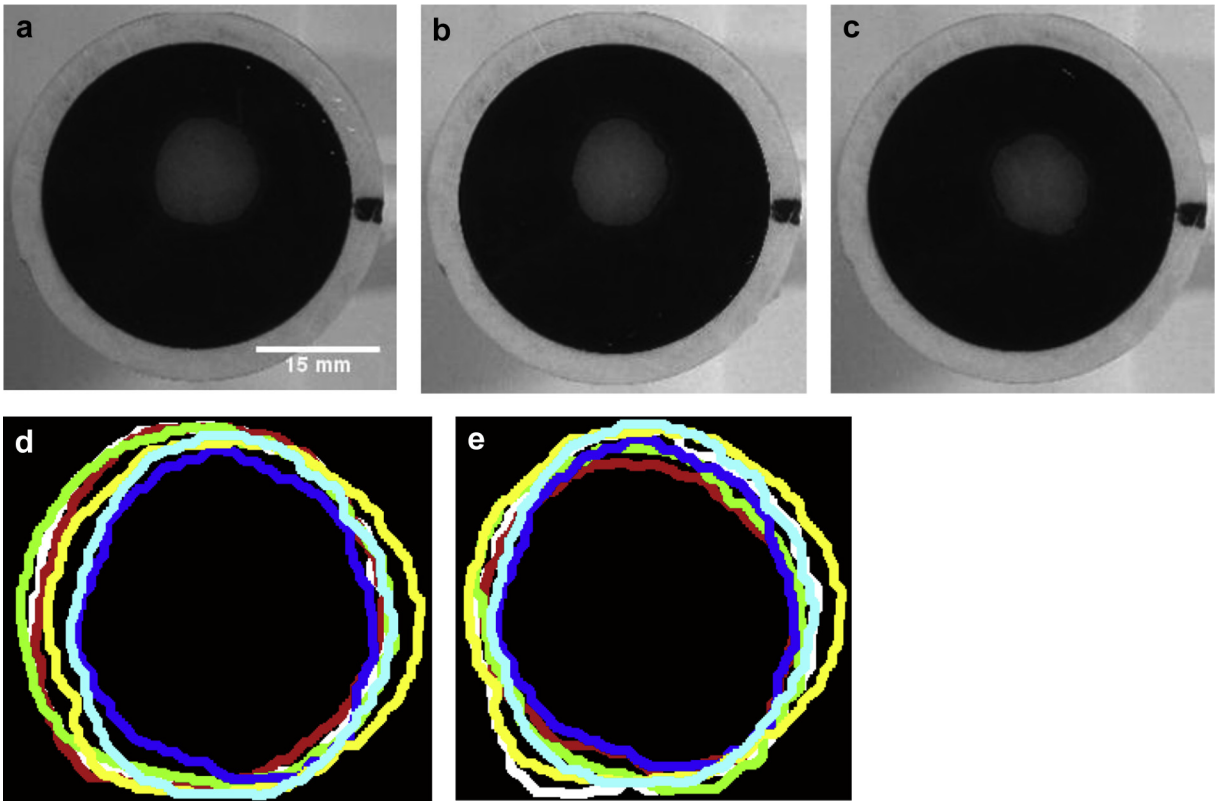

Fig. 5. (a) Example of a region heated in sample A4 achieved by operator 1, at second repetition, with transducer A. (b) Example of result obtained by operator 2 for the same sample A4. (c) Example of the heated area produced by a different sample (A3). (d) Area contours obtained from the three repetitions performed by operators 1 (*white, red and green*) and 2 (*blue, yellow and cyan*) for sample A4. (e) Area contours obtained by operator 1 using different samples (A3: *white, red and green*; A4: *blue, yellow and cyan*).

measurements of A_{ER} for transducer A tend to present high dispersion among the results obtained. This dispersion seems to be reflected in the results achieved using the thermochromic phantom.

General results indicate that different thermochromic phantom samples produce heated area values that are not statistically significantly different. In addition, no statistical difference is observed between the results achieved by two operators (Table 3) for all transducers. These results suggest that different thermochromic phantom samples have homogeneous behavior and tend to produce no statistically different results for a specific ultrasonic transducer assessed. Moreover, values of the heated area obtained for each transducer differ statistically, indicating that the thermochromic phantom samples have sufficient sensitivity to represent the heated areas of ultrasonic transducers with different characteristics.

The National Physical Laboratory (UK) has developed an acoustically absorbing tile containing a single thermochromic pigment, which changes color in response to the heating produced by the time-averaged intensity generated by ultrasound physiotherapy treatment heads (Butterworth et al. 2012). Zauhar et al. (2015) used the same thermochromic tile described by Butterworth et al. (2012) to estimate the effective radiating area of nine ultrasound physiotherapy treatment heads. They assumed that the local time-averaged acoustic intensity at each pixel is proportional to the square of

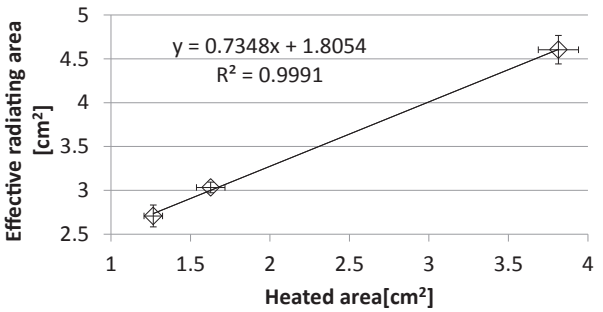

Fig. 6. Scatter plot revealing the relationship between heated area and effective radiating area. Vertical bars represent standard deviation from heated areas (see Table 4), and horizontal bars represent the combined uncertainties from effective radiating areas (see Table 1).

Table 2. Areas of the heated region for transducers A–C with respective standard deviations, achieved by operators 1 and 2

		Operator 1			Operator 2		
Transducer	Sample	Mean area (cm^2)	Standard deviation (cm^2)	Overlap ratio*	Mean area (cm^2)	Standard deviation (cm^2)	Overlap ratio*
A	1	1.23	0.05	0.88	1.19	0.13	0.76
	2	1.27	0.11	0.76	1.21	0.15	0.71
	3	1.26	0.04	0.79	1.23	0.15	0.75
	4	1.47	0.03	0.89	1.28	0.21	0.71
B	5	1.60	0.13	0.83	1.60	0.10	0.84
	6	1.64	0.01	0.89	1.68	0.06	0.83
	7	1.58	0.02	0.87	1.63	0.03	0.83
	8	1.63	0.03	0.87	1.65	0.05	0.84
C	9	3.96	0.13	0.93	3.73	0.10	0.94
	10	3.77	0.19	0.90	3.85	0.25	0.88
	11	3.89	0.19	0.89	3.75	0.16	0.91
	12	3.77	0.05	0.94	3.79	0.10	0.92

* Respective overlap ratio among the three repetitions for each sample is also presented.

the acoustic pressure integrated along the optical path. Then, they determined A_{ER} directly from the images acquired from the thermochromic tile using the calculation described in IEC 61689 (IEC 2013a). Zauhar et al. (2015) state that the differences between the A_{ER} values obtained experimentally and those specified by the manufacturer are lower than 25%, with the A_{ER} value obtained using the thermochromic material tending to underestimate the declared A_{ER}.

The heated area values obtained in our work are lower than the respective effective radiating area (A_{ER}) determined as described in IEC 61689 (IEC 2013a) using the field mapping facility (compare Tables 1 and 4). Hence, we believe that the proposed procedure cannot be employed for the direct determination of A_{ER}. However, the two values are highly correlated (Fig. 6), suggesting that the proposed procedure could be used as a quick test to qualitatively assess possible changes in system performance. The heating pattern could be recorded during the acceptance test of the ultrasound physiotherapy device and used as a reference for future tests. It is important to note that A_{ER} is not related to the output power of an ultrasound system, whereas the heating area, as proposed in the present work, is related to the output power. This is primarily the reason why the regression line in Figure 6 does not cross the (0, 0) point, that is, the origin of the coordinate system of the graph. Moreover, if the main parameters used in the proposed procedure (*e.g.*, insonation time and output power) vary, it is not possible to assume or theoretically preview the regression behavior.

The results in Table 4 indicate the importance of effectively using the entire evaluation procedure. Future tests should have results lying within the confidence interval of the mean values presented in Table 4. If a future test fails to accomplish this, one could suspect that the ultrasonic output of the equipment is not the same as it was during determination of the heated area values. This difference could be due to variation in its effective radiating area, its output power or both.

Zauhar et al. (2015) reported that the repeatability and reproducibility of results depend on the force applied to the treatment head coupling. To mitigate this issue, they proposed use of a weight of known mass in their work. However, this problem seems to be more pronounced in treatment heads with curved shapes, where it is hard to apply sufficient weight to achieve adequate repeatability. In our study, this problem did not exist because water was used as the coupling medium between the surface transducer and thermochromic phantom,

Table 3. Mean area of samples from the same group for each operator and respective standard deviations*

	Operator 1		Operator 2					
Transducer	Mean area (cm^2)	Standard deviation (cm^2)	Mean area (cm^2)	Standard deviation (cm^2)	F Tabulated ($\alpha = 0.05, n_1 = 11, n_2 = 11$)	F Calculated	t Tabulated ($\alpha = 0.05, n_3 = 22$)	t Calculated
A	1.31	0.11	1.23	0.14	3.5	1.59	2.4	1.48
B	1.62	0.06	1.64	0.07		1.09		0.88
C	3.85	0.16	3.78	0.15		1.10		1.09

* The calculated F-values are smaller than the F-tabulated value, indicating that the variances between the two operators are homogeneous, whereas the calculated t-values are smaller than the t-tabulated value, indicating that no statistical difference exists between the results achieved by different operators. n_1, n_2 and n_3 are the degrees of freedom for the tests.

Table 4. Mean areas obtained by combining the results from both operators and respective standard deviations at intermediate measurement precision

	Both operators	
Transducer	Mean area (cm^2)	Standard deviation (cm^2)
A	1.27	0.12
B	1.63	0.06
C	3.81	0.16

which facilitates the use of transducers with any surface shape. Nevertheless, the procedure described herein is applicable only if an adapter is used for each shape of the treatment head. Here, it is important to clarify that no standing waves were observed during the experiments once less than –17 dB of the signal was reflected (the acoustic impedance of the phantom was approximately 1.2 MRayl).

The present work used repeatability and intermediate precision measurement conditions rather than reproducibility (BIPM 2012). In this regard, a test body was studied for a specific application, including its homogeneity and short-term stability. Subjacent aspects such as the camera, illumination condition and room temperature would not influence the capability of the phantom to change its color in response to temperature rise. The results experimentally and statistically indicated the phantom's capability to reproduce its behavior in repeatability conditions.

Future work will involve additional studies applying the proposed procedure as a quick test to assess changes in ultrasonic beam cross-sectional shape during the lifetime of ultrasound physiotherapy systems. Another possible application of the thermochromic phantom is its use as a fast-track analysis tool in an ultrasonic transducer production line, eliminating the need for digital image analysis; however, further development is required to validate this application.

Acknowledgments—The authors acknowledge the financial support of the following Brazilian agencies: National Council for Scientific and Technological Development (CNPq) (Grant: 308.627/2013-0; 459.680/2014-5; 309717/2014-0), Carlos Chagas Filho Research Support Foundation (FAPERJ) (Grant: E-26/103.182/2011), Coordination for the Improvement of Higher Education Personnel (CAPES) and Programa de Capacitação Científica e Industrial do Inmetro (CNPq-PROMETRO) (Grant: 550099/2013-1).

REFERENCES

Artho PA, Thyne JG, Warring BP, Willis CD, Brismée JM, Latman NS. A calibration study of therapeutic ultrasound units. Phys Ther 2002; 82:257–263.

Beyer RT. Parameter of nonlinearity in fluids. J Acoust Soc Am 1960;32: 719–721.

Blackstock DT. Connection between the Fay and Fubini solutions for plane sound waves of finite amplitude. J Acoust Soc Am 1966;39: 1019–1026.

Bureau International des Poids et Mesures (BIPM). Evaluation of measurement data: Guide to the expression of uncertainty in measurement. JCGM 100. Available at: www.bipm.org/en/publications/guides/gum.html; 2008 (GUM 1995 with minor corrections).

Bureau International des Poids et Mesures (BIPM). International vocabulary of metrology: Basic and general concepts and associated terms. JCGM 200. Available at: www.bipm.org/en/publications/guides/vim.html; 2012 (VIM 3rd ed.).

Butterworth I, Barrie J, Zeqiri B, Zauhar G, Parisot B. Exploiting thermochromic materials for the rapid quality assurance of physiotherapy ultrasound treatment heads. Ultrasound Med Biol 2012; 38:767–776.

Cook BD, Werchan RE. Mapping ultrasound fields with cholesteric liquid crystals. Ultrasonics 1971;9:88–94.

Ferrari CB, Andrade MAB, Adamowski JC, Guirro RRJ. Evaluation of therapeutic ultrasound equipments performance. Ultrasonics 2010; 50:704–709.

Gómez W, Krüger MA, Pereira WCA, Leija L, Vera A. Analysis of SAR with thermochromic liquid crystal sheets in focused ultrasound beam. In: Proceedings, XX Brazilian Congress on Biomedical Engineering, CBEB 2006, São Pedro, Brazil, 2006:819–822. Available at: http://www.researchgate.net/profile/Marco_Antonio_Von_Kruger2/publication/228866635_Analysis_of_SAR_with_Thermochromic_Liquid_Crystal_Sheets_in_Focused_Ultrasound_Beam/links/547faa350cf250f1edbef930.pdf?inViewer=true&disableCoverPage=true&origin=publication_detail. Accessed October 7, 2015.

Guirro R, Santos SCB. Evaluation of the acoustic intensity of new ultrasound equipment. Ultrasonics 2002;39:553–557.

Hekkenberg RT, Oosterban WA, Van Beekum WT. Evaluation of ultrasound therapy devices. Physiotherapy 1986;72:390–395.

International Electrotechnical Commission (IEC). IEC 61689: Ultrasonics—Physiotherapy systems—Field specifications and methods of measurement in the frequency range 0.5 to 5 MHz. 3rd edition. Geneva: Author; 2013a.

International Electrotechnical Commission (IEC). IEC TS 61161: Ultrasonics—Power measurement—Radiation force balances and performance requirements. 3rd edition. Geneva: Author; 2013b.

International Electrotechnical Commission (IEC). IEC TS 62462 Ultrasonics – Output test – Guide for the maintenance of ultrasound physiotherapy systems. Geneva: Author; 2007.

Ishikawa NM, Alvarenga AV, Paes LFC, Pereira WCA, Machado JC. Performance analysis of ultrasound equipment for physiotherapy, operating in the city of Rio de Janeiro, according to ABNT NBR IEC 61689. Braz J Phys Ther 2002;6:63–69 [In Portuguese.].

Macedo AR, Alvarenga AV, Pereira WCA, Machado JC. Ultrasonic beam map using thermochromic properties of cholesteric liquid crystals. Braz J Biomed Eng 2003;19:61–68.

Martin K, Fernandez R. A thermal beam-shape phantom for ultrasound physiotherapy transducers. Ultrasound Med Biol 1997;23:1267–1274.

Merrick MA, Bernard KD, Devor ST, Williams MJ. Identical 3-MHz ultrasound treatments with different devices produce different intramuscular temperatures. J Orthop Sports Phys Ther 2003;33: 379–385.

Pye SD, Milford C. The performance of ultrasound physiotherapy machines in Lothian region, Scotland, 1992. Ultrasound Med Biol 1994;20:347–359.

Schabrun S, Walker H, Chipchase L. How accurate are therapeutic ultrasound machines? Hong Kong Physiother J 2008;26:39–44.

Soille P. Morphological image analysis. Heidelberg: Springer; 1999.

Speed CA. Therapeutic ultrasound in soft tissue lesions. Rheumatology 2001;40:1331–1336.

Zauhar G, Radojcic DS, Dobravac D, Jurkovic S. Quantitative testing of physiotherapy ultrasound beam patterns within a clinical environment using a thermochromic tile. Ultrasonics 2015;58: 6–10.